

1 **The role of edible oils in Low Molecular Weight**
2 **organogels rheology and structure**

3
4 *F. R. Lupi¹, M.P. De Santo^{2,3}, F. Ciuchi³, N. Baldino¹, D. Gabriele¹*

5
6 ¹ Department of Information, Modeling, Electronics and System Engineering,
7 (D.I.M.E.S.) University of Calabria, Via P. Bucci, Cubo 39C, I-87036 Rende (CS),
8 Italy

9 francesca.lupi@unical.it; domenico.gabriele@unical.it;

10
11 ² Department of Physics, University of Calabria, Via P. Bucci, Cubo 31C, I-87036
12 Rende (CS,) Italy

13
14 ³ CNR-NANOTEC c/o Department of Physics, University of Calabria, Via P. Bucci,
15 Cubo 33B, I-87036 Rende (CS) Italy

16
17 **Corresponding author**

18 Dr. Domenico Gabriele

19 Department of Information, Modeling, Electronics and System Engineering
20 (D.I.M.E.S.)

21 Via P. Bucci – Cubo 39C

22 I-87036 Arcavacata di Rende (CS), Italy

23 Email: domenico.gabriele@unical.it

24 Tel. +39 0984 496687; Fax +39 0984 494009

25
<https://doi.org/10.1016/j.foodres.2018.05.050>

© <2018>. This manuscript version is made available under the CC-BY-NC-ND 4.0 license

<https://creativecommons.org/licenses/by-nc-nd/4.0/>

26 **ABSTRACT**

27 In this paper, the role of solvent characteristics on the rheological and physicochemical
28 properties of organogels was investigated using different techniques. Vegetable oils, such
29 as rice, sunflower and castor oil were used as solvents, for producing organogels with
30 monoglycerides of fatty acids or a mixture of fatty alcohols (policosanol) as gelators.
31 Moreover, two non-edible oils (silicon and paraffin oil) were also used for analysing the
32 properties of solvents completely different in nature with respect to the edible ones, for a
33 better interpretation of the given results. Organogels were investigated from a rheological
34 point of view and through a microscopic analysis, given by polarised light (POM) and
35 atomic force (AFM) microscopy, and X-rays to study the crystallinity of the system. The
36 IR technique was used to analyse the intermolecular interactions, resulting in interesting
37 information about the effect of oil polarity on the driving forces promoting structuration.
38 This investigation showed that when solvents of a similar chemical nature are used, their
39 physical properties, mainly oil polarity, are strictly related to the properties of the
40 organogel, such as the onset of crystallisation temperature, the stiffness of the final
41 material and its crystallinity. Anyway, these physical parameters seem insufficient to
42 describe properly the role of solvents when oils of a different chemical nature are
43 compared.

44 **Keywords:** *organogels; polarity; rheology; X-ray; Interfacial Tension (IFT); Atomic*
45 *Force Microscopy (AFM); Fourier Transform Infrared Spectroscopy (FTIR); Polarised*
46 *Optical Microscopy (POM)*

47

48 1. INTRODUCTION

49 Low molecular weight (LMW) organogels are soft solids with gel characteristics, where
50 an organic solvent (typically an oil) is structured thanks to the self-assembly action of
51 LMW organogelator molecules, mainly interacting among themselves with weak
52 interaction such as H-bonds or van der Waals forces (Lupi et al, 2016; Lupi et al, 2017;
53 van Esch & Feringa, 2000). Organogels are very interesting for their potential uses in
54 different fields; in particular, in the food industry, they are used for replacing saturated
55 and hydrogenated fats with a healthier lipid phase (Marangoni & Garti, 2011). The main
56 characteristics of organogels have been deeply investigated by research, in particular the
57 rheological properties (Calligaris et al, 2014; Chaves et al, 2017; Co & Marangoni, 2012;
58 Lupi et al, 2012; Lupi et al, 2013; Morales-Rueda et al, 2009; Ojijo et al, 2004), the
59 microstructural arrangements of crystals (Schaink et al, 2007; Toro-Vazquez et al, 2013),
60 and also the weak interactions which give particular properties to these systems (Lupi et
61 al, 2016; Zweep et al, 2009). An interesting topic not yet completely investigated is the
62 effect of the solvent on these properties. In particular, it is remarkable to understand how
63 the chemical characteristics of the solvent can affect the consistency, the structuration,
64 but also the strength of the interactions among crystals and the thermorheological
65 parameters (T_{co} , onset of crystallisation temperature and T_g , gelation temperature) of
66 these materials, keeping constant the quantity and the kind of organogelator. On this topic,
67 an interesting work was published by Calligaris et al. (2014) on the effect of oil type
68 (viscosity and polarity) on the firmness and thermal properties of samples prepared with
69 sitosterol and γ -oryzanol. The authors found that highly-viscous and polar solvents gave
70 less structured organogels; according to the authors, this can be attributed to the increased
71 difficulty of β -sitosterol and γ -oryzanol molecules to pack together as the oil viscosity

72 increased, whereas the increased polarity of the solvent could change the solvent-gelator
73 interaction, lowering gelator-gelator interaction as a consequence. A similar study was
74 carried out by Sawalha et al. (2013) for organogels structured with the same gelators.
75 They measured oil polarity through the evaluation of the dielectric constant; according to
76 the authors, polarity increases if the dielectric constant also increases. With their work,
77 the authors concluded that fibres constituting the network were more stable, decreasing
78 the polarity of the oil. Moreover, the gels prepared with polar oils, i.e. sunflower oils and
79 eugenol, were generally transparent, whereas gels prepared with low polarity oils were
80 opaque after a short time of preparation. Recently, in an interesting work, Hwang et al.
81 (2014) investigated the effects of polar compounds and fatty acids profile on macroscopic
82 properties of organogels and margarines prepared with sunflower wax and different
83 edible oils; the authors did not observe a clear relation between the firmness of obtained
84 systems and amount of polar compounds and fatty acids, concluding that, even if some
85 organogel properties could be dependent on them, other factors probably play a relevant
86 role (such as the position of fatty acids on the glycerol units or minor components).

87 According to Zhu and Dordick (2006) and Wu et al. (2013) the structuration of LMW
88 organogels is a result of the nature of gelator-gelator and solvent-gelator interactions, and
89 this process involves specific and nonspecific intermolecular forces (H-bonds and weak
90 interactions). Moreover, the network formation is dominated by the polarity of the solvent
91 and the hydrophobic/hydrophilic characteristic of the gelator. In general, according to the
92 authors, gelation is better achieved by using a solvent that has limited interaction with the
93 organogelator, because restricted solvent-gelator interaction enhances the growth of thin
94 and highly branched fibres, leading to stronger and more stable gels. On the contrary,
95 strong solvent-gelator interactions allow the clustering of gelator aggregates, resulting in

96 less stable gels. Therefore, gelation process can be properly tuned by adjusting the solvent
97 polarity with the addition of cosolvents to a gelator solution at room temperature. Zweep
98 et al. (2009) investigated the effect of the solvent-gelator interactions, concluding that
99 polar solvents allow the formation of weak H-bonds and hence gelation occurs if a
100 sufficient compensation is provided by the van der Waals interactions contribution.
101 Therefore, the authors concluded that in polar solvents structuration, van der Waals
102 interactions play a dominant role, whereas in apolar solvents H-bonding interactions
103 dominate. Similar results were also described by de Vries et al. (2017), who investigated
104 the effect of protein aggregates in structuring vegetable oils (extra virgin olive oil,
105 sunflower oil and castor oil) with different polarities. The authors found that gel strength
106 is affected by the polarity of the solvent, and weaker gels are built in more polar oils, as
107 a result of larger gelator solvent interactions. Currently, despite the efforts made in finding
108 the exact process occurring during organogelation, a scarce literature is currently
109 available on the role of commercial edible oils as solvents interacting with gelators for
110 oleogel formation. In the present work, a deep understanding of the interactions among
111 different edible oils with commercial organogelators (monoglycerides of fatty acids,
112 MAGs, and policosanol, a mixture of fatty alcohols) is presented, in an attempt to
113 investigate the rheological and microstructural characteristics of gels produced with them.
114 Edible oils investigated in this work are sunflower oil, rice oil and castor oil (to be
115 assumed in a small amount, according to the Food Agricultural Organization (Johnson,
116 2007)). In addition a mineral oil, i.e. paraffin oil, and silicon oil were also studied as a
117 sort of benchmark having chemical characteristics different with respect to those of
118 triglycerides systems (even if some physical properties are similar).

119

120 2. MATERIALS AND METHODS

121 2.1 Materials

122 Different oils were used to examine the effect of the solvent on the properties of
123 organogels. In particular, organogels were prepared with sunflower oil ‘SO’ (Fabiano,
124 Italy), castor oil ‘CO’ (Sigma-Aldrich, Germany), rice oil ‘RO’ (Dr. Taffi, Italy), paraffin
125 oil ‘PO’ (Sigma-Aldrich, Germany) and silicon oil ‘SiO’ (VWR Chemicals, France).

126 Two kinds of LMW organogelators were used: a mixture of fatty alcohols (policosanol,
127 ACEF, Italy) (Lupi et al, 2016; Lupi et al, 2017) and distilled monoglycerides of saturated
128 fatty acids (with an equal mass fraction of glyceryl monostearate and glyceryl
129 monopalmitate) prepared from kosher palm feedstock and glycerol (Myverol 18 04 K,
130 Kerry group, Ireland). All reactants were used without further purification. The physical
131 properties of the oils are described in table 1 and the methods used for their analysis are
132 described in detail in section 2.3.

133 2.2 Samples preparation

134 All organogels were prepared with the same amount (5% w/w) of Myverol, and only for
135 silicon oil, one organogel sample was produced also with the same amount of policosanol.
136 Samples were prepared following the procedure already described in previous works
137 (Lupi et al, 2016; Lupi et al, 2017). The oil was stirred continuously with an overhead
138 stirrer (RW 20, IKA-Werke, Germany) and it was warmed up to 70°C or 85°C according
139 to the different organogelator used (70°C for MAGs organogels and 85°C for policosanol
140 organogels) with a thermostated water bath (Arex, Velp scientific, Italy). Organogelator
141 was added to the hot oil, stirring for a further 10 minutes to guarantee the complete
142 melting of the gelator before starting the measurements. Organogel samples are labelled,

143 in the text, with two letters, the first one indicating the initial of the oil ('S' for sunflower
144 oil, 'C' for Castor oil, 'R' for rice oil, 'P' for paraffin oil and 'Si' for Silicon oil), and the
145 other one related to the organogelator used ('M' for Myverol and 'P' for Policosanol).

146

147 **2.3 Pure oils characterisation: viscosity, interfacial tension, dielectric constants and** 148 **fatty acids profile**

149 Oils were characterised with different techniques aiming at better understanding the
150 potential effects of an organogelator on different solvents. First of all, the rheological
151 properties of oils were investigated performing Step Rate Temperature Ramp tests
152 (SRTRTs) with the controlled stress rheometer MARS III (Thermo Scientific, Germany)
153 adopting a parallel plates geometry (P50 Ti L, diameter 50 mm, gap= 1 ± 0.1 mm) and a
154 Peltier system for temperature control. A constant value of shear rate of 10 s^{-1} was used
155 and the tests were carried out from 70°C (only for silicon oil, used to prepare policosanol
156 organogels, tests started at 80°C) down to 10°C with a cooling rate of $1^\circ\text{C}/\text{min}$. All
157 samples were examined three times and experimental results are shown in terms of
158 average values and standard deviation.

159 Transient interfacial tension profiles of oils, at water interface, were measured with the
160 automated pendant drop tensiometer FTA200 (First Ten Angstrom, USA, software of
161 analysis Fta32 v 2.0). The Axisymmetric Drop Shape Analysis (ADSA) was used to
162 calculate drop volume, area and interfacial tension profile (Seta et al, 2014). A water
163 droplet (twice-distilled water obtained from a Milli-Q purification system (Millipore,
164 USA)) of a volume of $30 \mu\text{L}$ was forced to be formed inside a quartz cuvette containing
165 the oil to be tested; images were taken every 10 s for a total time of 120 min. A quasi-

166 equilibrium value of interfacial tension (IFT) was assumed when change with time was
167 lower than 0.5 mN/m in 30 min. The analysis procedure is described in detail by Seta et
168 al. (2012).

169 The relative dielectric constant of oils (ϵ_r') was also analysed, since it can be considered
170 an indirect measurement of oil polarity (Sawalha et al, 2013; Wang, 2011). The dielectric
171 constant was inferred from Complex Impedance measurements acquired at room
172 temperature by a potentiostat/galvanostat/impedentiometer EG&G model 273A in
173 frequency range 0.1-10⁵ Hz. In the experimental set-up, a wire acted as working electrode,
174 whereas the counter electrode was short-circuited with the reference wire. The amplitude
175 of the sinusoidal applied voltage, $V_0 = 1000$ mV_{rms}, was chosen because measurements
176 at lower voltages give the same results but introduce more noise. Two gold electrodes
177 were evaporated on glass substrates, then glasses were assembled with two 12 μ m mylar
178 spacers: the active area of the cells (inner surfaces coated with gold) was $A \sim 1$ cm². The
179 thickness was checked by the interferometric method with an AVANTES (200-1000 nm)
180 spectrophotometer. Finally, the cell was filled with oil by capillarity. From complex
181 impedance measurements the real part of the relative dielectric constant at different
182 frequency is obtained using Eq. 1, modeling the cell as a circuit formed by a Resistance
183 and a Capacity (Barsoukov & MacDonald, 2005):

184
$$\epsilon'_r = \frac{Z_{im}}{Z_{real}^2 + Z_{im}^2} \frac{d}{A2\pi f} \quad (1)$$

185 Z_{im} and Z_{real} are the imaginary and the real part of the measured impedance, respectively,
186 d is the cell thickness, A the electrode area and f the frequency.

187 FT-NIR (Fourier Transform Near Infrared) spectroscopy is a technique already used for
188 investigating the acidic profile of vegetable oils, as deeply discussed by Azizian and
189 Kramer (2005), Casale et al. (2012), Galtier et al. (2007) based on the creation of an
190 average absorption file for (several) reference vegetable oil samples, used in the
191 development of a classification or quantification model. These models were then used to
192 classify oils having a similar Fatty Acids (FA) composition at a 99% confidence interval
193 or to quantify for FA composition.

194 The fatty acids content of vegetable oils was measured with an FT-NIR spectrometer
195 (MPA, Bruker, Germany), previously calibrated through the investigation of a wide
196 number of vegetable oils used as references, aiming at evaluating the properties of
197 solvents as a function of the Fatty Acids content (SFA Saturated Fatty Acids, Mono-
198 Unsaturated Fatty Acids, MUFAs, and Poly-Unsaturated Fatty Acids, PUFAs). The oil to
199 be tested was simply filled at room temperature into an 8 mm glass vial, and measured in
200 the sample compartment of the spectrometer. The OPUS software (Bruker Optics, USA)
201 was used to collect and handle the experimental data with a chemometric analysis.

202

203 **2.3 Organogel characterisation: rheological investigation, FTIR spectroscopy, X-** 204 **rays, Polarization Microscopy, Atomic Force Microscopy**

205 The rheology of organogels was investigated with a controlled strain rheometer (ARES
206 RFS, TA Instruments, USA, parallel plates 50 mm, gap 1.0 ± 0.1 mm). Preliminarily,
207 strain sweep tests were carried out at different constant temperatures from the preparation
208 value, i.e. 70 °C or 80° when policosanol was used, down to 10 °C almost every 10 °C to
209 investigate potential changes in the linear viscoelastic region.

210 Dynamic temperature ramp tests were performed at 1 Hz in the linear viscoelastic regime,
211 cooling the sample from the starting temperature of preparation down to 10 °C with a
212 cooling ramp rate of 1 °C/min. Even in this case, all samples were examined three times
213 and experimental results are shown in terms of average values and standard deviation.
214 Observed average error was lower than 10%, larger deviations were seldom observed for
215 data at high temperature, owing to instrument limits, or in the transition crystallization
216 region, owing to the fast structuring phenomena.

217 The onset of crystallization (T_{co}) was defined as the temperature corresponding to the
218 sudden increase of complex modulus G^* (or the abrupt decrease of the loss tangent curve)
219 in temperature ramp as already discussed in previous papers (Lupi et al, 2013).

220 The gelation temperature (T_g), that is, the temperature at which crystal clusters or fibres
221 of organogelators begin to interconnect, was evaluated as the temperature corresponding
222 to the crossover of dynamic moduli (phase angle equal to 45°) (Lupi et al, 2012).

223 The weak interactions, thanks to which the organogel is formed, were analysed with a
224 Fourier Transform Infrared Spectroscopy (FT-IR Nicolet IS-10, Thermo Scientific,
225 USA), equipped with a sampling accessory smart Itr ATR (attenuated total reflectance,
226 data spacing 0.482 cm⁻¹, 64 scans for each test). The same tests were also carried out for
227 pure oils to have a comparison of gels properties with respect to solvents. Organogels
228 made for these investigations were prepared as previously described, and afterwards
229 cooled down to room temperature. Once the gels were formed, an average sample amount
230 of 20 mg was loaded into the instrument to be analysed.

231 An Atomic Force Microscope (AFM), Multimode 8 equipped with a Nanoscope V
232 controller (Bruker), was used to have an inspection of the topography of samples on a

233 length scale varying from few nm to one hundred of μm . Organogels were deposited using
234 a spatula on a sample holder and heated to temperatures higher than their melting point
235 to allow the sample to spread and rearrange over the surface creating an almost flat
236 air/organogel interface. Then, samples were cooled down to 25°C in a thermostatic water
237 bath (F25, Julabo, USA). The samples surface was investigated operating the AFM in
238 Tapping mode and using levers with a resonance frequency of 300 kHz and a tip nominal
239 radius of curvature of 10 nm (RTESPA, Bruker). All the measurements were performed
240 in air and at room temperature.

241 X-rays analysis was carried out with a D8 Discover reflectometer (Bruker axs),
242 wavelength of 1.5418 \AA . This instrument was set for transmission measurements with a
243 capillary holder made expressly for these tests. Capillaries had an inner diameter of 1 mm
244 and an outer diameter of 1.01 mm.

245 For these tests organogels were warmed up to temperature values higher than their
246 melting points, and then poured into capillaries. Afterwards, the capillary was
247 thermostated and cooled down to 25°C with a controlled cooling rate of $1^{\circ}\text{C}/\text{min}$ in order
248 to guarantee the same thermal history used in rheological tests. For each samples, there
249 were two intervals of measurements: 0.8-10 and 19-25 in 2θ ($(\Delta(2\theta))=0.004$ scan,
250 velocity= 2 s/step).

251 A Polarized Optical Microscope (POM, Digital-Modul-R Leica, Germany), was used to
252 point out the presence of small birefringent crystalline structures inside the organogels.
253 Samples were prepared confining a small amount of the material between two glass slides,
254 using the same thermal treatment as described previously, and imaged at room
255 temperature between crossed polarizers.

256

257 **3. RESULTS AND DISCUSSION**

258 **3.1. Characteristics of pure oil**

259 Pure oils were characterised to understand their effect on the final properties of
260 organogels. Temperature ramp tests (data not shown) evidenced a gradual monotonous
261 increase, with decreasing temperature, without sharp and sudden changes which would
262 be present in case of crystal formation (as it occurs in organogels), this further confirms
263 that oils are liquid within the investigated temperature range. Vegetable oils (SO, CO and
264 RO) are a mixture of triglycerides of fatty acids, which, in turn, are different among
265 themselves. In fact, the three oils are characterised by a different acidic profile, and their
266 fatty acid contents are different; their value is listed in table 1. It is worth noticing that oil
267 viscosities at 25°C decrease with the increase of PUFAs, as shown in Tab. 1. This was
268 expected, considering that the unsaturation of fatty acids attached to glycerol in
269 triacylglycerols allows a higher mobility of the carbon chain, and a bigger steric hindrance
270 which reduces molecular density and oil viscosity as a consequence (Quinchia et al,
271 2012). Moreover, according to Quinchia et al. (2012), the concentration of PUFAs affects
272 the low-temperature viscosity of oils more than the concentration of the other saturated
273 fatty acids.

274 The relative dielectric constant decreases with the following order CO>RO>SO, whereas
275 IFT increases up to a plateau value (SO>RO>CO) therefore it can be noticed that, for
276 vegetable oils, IFT decreases when ε'_r increases (Table 1). It is well-known from the
277 literature that oils have different compositions in terms of impurities such as
278 unsaponifiable lipids, tocopherols, sterols, oryzanol, humidity and so on (Grompone,

279 2011; Kochhar, 2011). This polar “impurities” are mainly responsible for the interfacial
280 activity of oils. Therefore, even if three points are not sufficient to draw conclusions about
281 the material behaviour, it could be speculated that polar compounds, able to increase the
282 polarity of rough oils are also responsible for lowering their interfacial tension.

283 The other two oils chosen for producing organogels were not vegetable, and in fact, they
284 were chosen to understand the effect of oils completely different in nature. Paraffin oil is
285 a mixture of n-alkanes with a very little content of impurities, whereas silicon oil is a
286 polydimethylsiloxane: both of them are characterised by the same value of the dielectric
287 constant (average values overlap within the experimental error range, see table 1) but with
288 different values of interfacial tension. Therefore, it can be speculated that for synthetic
289 oils the interfacial properties are not a function of the dielectric constant, since both these
290 oils do not contain significant amounts of impurities.

291 **3.1. Characteristics of organogels: rheology**

292 Myverol (5% w/w) was used to prepare organogels with all oils, whereas policosanol (in
293 the same amount) was used only with silicon oil (Table 2) to investigate the effects, on
294 non-edible oils, of one gelator which proved to self-assemble in olive oil with a
295 mechanism different than that observed for Myverol (Lupi et al, 2016). Figure 1 shows
296 the dynamic temperature ramp tests of all samples prepared with Myverol in terms of G^*
297 (Fig. 1a) and phase angle, δ , (Fig. 1b) as a function of temperature. At high temperatures,
298 all samples are molten and behave as purely viscous liquids as shown by the phase angle
299 value close to 90° (Fig. 1b). All organogels, in their molten state, show similar values of
300 complex moduli (Fig. 1a) except for sample CM that has values greater than the others.
301 This, apparently, is in contrast with previous literature results (Lupi et al, 2012) where it

302 was observed that the viscosity of the solvent did not affect the rheological properties of
303 the derived organogels in the molten state. Anyway, it is worth noticing that castor oil
304 viscosity is one order of magnitude greater than the others, therefore it can be concluded
305 that differences in molten organogels reflect potential differences in oils, and cannot be
306 appreciated only when pure oil viscosities are similar (as in the case of sunflower and rice
307 oil).

308 At the T_{co} , a sudden increase of moduli, and a decrease of phase angle, indicate the
309 beginning of crystallisation. This value depends on the solvent and it decreases with
310 decreasing IFT and with increasing ϵ'_r (see fig. 2) for all investigated oils that exhibit
311 crystallisation phenomena; in fact it is worth noticing that for silicon oil no crystallisation
312 appears in the investigated range of temperature. Similar results were described by
313 Sawalha et al. (2013) and Calligaris et al. (2014), according to which a decrease in oil
314 polarity lead to a higher structuring temperature, and a self-assembly action of
315 organogelator shaped as tubules. Even the viscosity of the solvent strongly affects the
316 properties of the resulting organogel. Table 2 shows the relationship between the T_g of
317 organogels and the solvent viscosity evaluated at T_g , evidencing a marked decrease of T_g
318 with increasing solvent viscosity. The effect of oil viscosity on organogel properties was
319 already investigated for different organogelators reporting results similar to those
320 observed in the present work; Calligaris et al. (2014) investigated the effect of oil
321 characteristics on β -sitosterol and γ -oryzanol organogels and they found that solvents
322 characterised by different dielectric constants (polarity) and viscosity showed different
323 gelling kinetics, as well. Castor oil (the most polar and viscous oil used by those authors),
324 for example, did not even gel after three months of investigation, whereas the other
325 vegetable oils, all less viscous and polar, required less than 1 h. According to the authors,

326 who confirmed what was already found by Bot et al. (2006; 2008), the formation of the
327 gel network is the results of two steps: the first one is the self-aggregation of
328 organogelator molecules into tubules and the second one is the junction of tubules
329 forming the network itself. The increase in oil viscosity can decrease the rate of collision
330 between molecules first and tubules later on, delaying the whole process.

331 Aiming at relating the rheological properties of organogels to physical properties of the
332 solvent, complex modulus and phase angle were plotted as a function of dielectric
333 constant. Anyway, if only the effects of organogelator-oil interactions have to be
334 investigated, data have to be independent of potential differences in liquid oils rheological
335 properties.

336 When organogel data at temperature higher than T_{co} are considered (see Fig. 1a) it can
337 be noticed that the complex modulus increases slowly with decreasing temperature
338 evidencing an almost linear trend in semi-log scale; in these conditions, where crystals
339 are not yet present, the system behaves as a viscous liquid and complex modulus increases
340 only because of a decrease in molecular mobility (Lupi et al, 2011). As a consequence, a
341 simple exponential model (analogous to the Andrade equation used to fit edible oil
342 viscosity (Noureddini et al, 1992)) can be used to describe complex modulus variation
343 with temperature between T_{co} and 70°C for each system (Eq. 2):

344
$$G_0^*(T) = A \cdot \exp^{\frac{B}{T}} \quad (2)$$

345 where A and B are fitting parameters depending on the specific investigated oil. It can be
346 assumed that, if crystal formation would not occur at T_{co} , eq. 2 could be suitable to
347 describe material behaviour even at lower temperature, therefore it can be used to
348 extrapolate, at temperature lower than T_{co} , the complex modulus of a hypothetical non-

349 gelled system. Starting from these considerations a dimensionless complex modulus (G_s^*
350) was defined as the ratio between the complex modulus of the organogel G^* , and the
351 extrapolated complex modulus of a non-gelled oil-organogelator system, G_0^* , at the same
352 temperature obtained with eq. 2:

$$353 \quad G_s^*(T) = \frac{G^*(T)}{G_0^*(T)} \quad (3)$$

354 Being G_0^* dependent on the specific oil, the dimensionless modulus G_s^* should be
355 function of organogelator-oil interactions, only. A similar evaluation of a dimensionless
356 phase angle was not necessary because the non-gelled reference (δ_0) is the same for all
357 systems (i.e. approximately 90°). All moduli were evaluated at a constant distance from
358 the onset of crystallisation, i.e. $T_{10} = T_{co} - 10^\circ\text{C}$.

359 Figure 3 depicts the trend of G_s^* with the dielectric constant, evidencing a marked
360 decrease of data with the increase of solvent polarity. A different trend is found if δ is
361 analysed: apparently, a minimum in the curve seems present, which hypothetically should
362 correspond to a maximum of the structuration degree. Nevertheless, the error bar is quite
363 large, with respect to the differences, and this suggests considering constant the phase
364 angle, although further investigations on this topic could be necessary.

365 An interesting discussion can be carried out if the systems prepared with silicon oil and,
366 in turn, Myverol or policosanol are taken into account. The dynamic temperature ramp
367 tests of samples SiM and SiP are shown in figure 4 in terms of complex modulus and
368 phase angle. As it can be noticed, a huge difference distinguishes the two samples: the
369 former is not crystallised or gelled in the whole range of investigated temperatures (δ is

370 about 90° in the whole range of temperature), whereas the latter is a gel starting from very
371 high temperatures ($74.2 \pm 0.2^\circ\text{C}$), and it shows elastic properties and a strong
372 structuration.

373 This evidence suggests a potentially different role of the solvent in promoting or
374 disadvantaging gelator-gelator interactions. Consequently, a deeper investigation was
375 carried out with FT-IR tests in an attempt to better understand the nature of these
376 interactions (see section 4.2).

377 Summarising the results so far discussed, it can be concluded that if organogels based on
378 oils made of triglycerides (i.e. vegetable oils) are considered a clear trend between
379 organogel properties (such as T_{co} , T_g , complex modulus) and pure oil physical properties
380 (polarity or interfacial tension) is found. This is probably caused by the similar molecular
381 structure of these oils containing esters derived from glycerol and fatty acids differing
382 among them for the number of carbon atoms and unsaturated bonds, but having the same
383 structure. On the other hand, when other investigated solvents are considered, a more
384 complex behaviour is observed, in fact data obtained for paraffin oil, a mixture of alkanes,
385 are in good agreement with the trend previously discussed. This could be ascribed to the
386 similar molecular structure of the oils where the linear chains are always based on carbon-
387 carbon bonds: differences with respect to vegetable oils arise mainly in the absence of
388 unsaturated bonds and of glyceryl units.

389 On the contrary, silicon oil based on chain consisting of alternating silicon and oxygen
390 atoms with side chains, exhibit a very different behaviour: it is not gelled by used Myverol
391 fraction within the considered temperature range, although the physical properties of this
392 oil are not so different from those of other solvents. This highlights that physical

393 parameters, such as polarity, are useful to classify solvents within a "chemical family"
394 (e.g. based on similar polymer chains like triglycerides are) but they seem to lose
395 relevance when materials with different chemical nature are used (for instance comparing
396 solvents based on carbon-carbon chains and silicon-oxygen ones). The solvent viscosity
397 seems to affect strongly the properties of the resulting organogel: in fact, a marked
398 decrease of T_{co} and gelation temperature, T_g , with increasing solvent viscosity was
399 found. Anyway it is worth noticing that, for investigated oils (except for silicon oil), a
400 monotonous relation between viscosity, IFT and ϵ'_r , was observed making difficult the
401 identification of potential single specific effects.

402 **4.2 FTIR tests**

403 IR tests were carried out to provide a microstructural interpretation of the effect of the
404 solvent on the rheological properties of organogels. The ability of an organogelator to
405 produce the network is due to the formation of weak interactions such as H-bonds and/or
406 van der Waals forces (van Esch & Feringa, 2000). The wavenumber region between 2500
407 and 4000 cm^{-1} corresponds to the OH-stretching vibrational modes, and it is particularly
408 interesting because monoglycerides have two OH groups in the hydrophilic part of the
409 molecule, whereas policosanol (for a sample produced with this gelator) has just one OH
410 group (Chen & Terentjev, 2009; Lupi et al, 2017). According to the literature, in the case
411 of long alkyl chains organogelators, van der Waals forces play also an important role in
412 creating the network (van Esch & Feringa, 2000; Wu et al, 2011). According to Suzuki et
413 al. (2003), van der Waals interactions can be detected in IR spectra as a shift of the
414 absorption bands of symmetric and anti-symmetric CH_2 stretching vibrational modes to
415 lower wavenumber. In particular, for vegetable oils, van der Waals interactions are

416 highlighted by the shift of the two peaks appearing in the wavenumber region around
417 2800 and 3000 cm^{-1} (Lupi et al, 2016).

418 On the basis of the gelator and solvent nature, both forces, or just one of them, can be
419 established. For example, Figure 5 shows the IR spectrum of pure silicon oil compared to
420 those of both organogels based on this oil. In the wavenumber region, where both the
421 cited weak interactions can be found, a broad peak between 3000 and 3800 cm^{-1} appears
422 in the spectrum of sample SiP, whereas it does not appear either in the sample produced
423 with Myverol or in the spectrum of pure silicon oil. As already remarked, the broad peak
424 with a shoulder correspondent to a wavenumber region of about 3500 cm^{-1} can be referred
425 to the vibration of OH groups; the shift of this peak towards lower wavenumber values
426 should indicate the formation of H-bonds between organogelator molecules (Chen &
427 Terentjev, 2009; Lupi et al, 2016; Lupi et al, 2017). On the other hand, the peaks
428 corresponding to the vibration of CH_2 groups, where, potentially, van der Waals
429 interactions could be detected, appear at the same wavenumbers (i.e. 2962 cm^{-1} and 2905
430 cm^{-1}) for all three samples. Therefore, it can be concluded that the leading force for
431 producing the network with policosanol and silicon oil as the solvent is just the H-bonds
432 formation. This behaviour is quite different with respect to what observed in previous
433 works (Lupi et al, 2016; Lupi et al, 2017) where the spectra of organogels produced with
434 olive oil and policosanol were analysed. In these cases, the predominant interactions
435 between gelators responsible for network formation were van der Waals forces, whereas
436 H-bonds appeared only if a great amount of policosanol (at least 8%w/w) was added to
437 the oil. In different organogels (Zweep et al, 2009) it was observed that, with increasing
438 oil polarity, van der Waals interactions become essential in structure formation, therefore
439 it could be speculated that differences observed between silicon and olive oil are caused

440 mainly by their distinct chemical nature, more than by simple differences in physical
441 properties.

442 Similar results were found for the other investigated samples, for which the H-bonding
443 was found to be the leading force. It is worth reminding that, in addition to the shift of
444 peaks, related to the presence of interactions, their intensity can give interesting
445 indications about the “quantity” of links formed during gelation (Brulls et al, 2007; Parolo
446 et al, 2017). In fact, it is known that band intensity indicates the amount of functional
447 groups responsible for IR absorption. From this point of view, figure 8 shows the peak
448 area (i.e. the area under the curves) correspondent to the OH groups’ vibration, for all the
449 investigated gels produced with Myverol. It is clear that, for vegetable oils (in Fig. 6 the
450 value for Paraffin oil is properly highlighted), the broadness of the H-bond peak increases
451 with the dielectric constant, i.e. the polarity of the solvent suggesting a direct relationship
452 between polarity and intensity of intermolecular interactions.

453

454 **4.2 Microscopic characterization of organogels**

455 Organogels prepared with Myverol were also tested with X ray diffraction, AFM and
456 POM. X rays spectra of samples are shown in Fig. 7. Sample SM is characterised by a
457 well-defined peak at low angle and one at high angle that can be attributed to Myverol
458 (Calligaris et al, 2010; Marangoni et al, 2007); moreover two broad bands, typical of oil
459 (Calligaris et al, 2010), were observed in both low angle (approximately around 4°) and
460 high angle region (between 19° and 20°). From the angle peak’s width, it is possible to
461 estimate sample crystallinity in order to compare the different samples. The RM sample
462 shows a low angle spectrum similar to that of SM, whereas at a high angle the peaks are

463 less visible, indicating an increased disorder in Myverol chains. The long-range order
464 crystallite dimension is similar to the previous one. Broad bands similar to those observed
465 in SM are present also in this case and can be attributed to the oil contribution. The X-ray
466 diffraction low angle peak in PM is well defined, broad bands are not visible in this case
467 due to the different nature of paraffin oil, while the high angle shows three peaks, i.e. an
468 increased order of Myverol chains. The long-range order crystallite dimension is similar
469 to the previous one. Sample CM shows quite different behaviour: the low angle peak is
470 enlarged and reduced in the intensity and the broad band at low angle seems shifted to
471 higher values; in addition, the high angle peaks are not visible. The castor oil-Myverol
472 interaction seems to induce a change in both the long range and short range Myverol
473 order. The crystallite dimension is hence reduced.

474 It is worth noticing that differences in the high angle region highlight the dissimilarities
475 in MAGs crystalline phase (Calligaris et al, 2010; Marangoni et al, 2007) among gels
476 prepared with different oils.

477 For what it may concern the silicon oil organogel, its spectrum is noisy since silicon oil
478 strongly absorbs CuK α X rays due to Si content. Nevertheless, in the high angle region a
479 peak is clearly visible and it can be attributed to policosanol, according to literature data
480 (Kim et al, 2015).

481 It is worth noticing that the width of low angle peaks increases in the order SiP-CM-RM-
482 SM-PM, as well as the trend of increase of complex modulus G^* of gels at 25°C (see Fig.
483 1a for confirmation). As foreseeable, an increase in crystallinity coincides with the
484 increase of complex modulus of gels.

485 Every POM image (Fig. 8) shows birefringent structures that appear strongly
486 interconnected, especially for SM, PM and RM. In CM samples, the birefringent areas
487 are less interconnected suggesting a looser structure. This is in agreement with rheological
488 data evidencing that CM samples are characterized by higher values of phase angle at
489 room temperature (approximately 20°) with respect to other organogels (close to 9° for
490 RM, SM and PM) and therefore exhibit a lower solid-like behaviour.

491 AFM (Fig. 9) confirms X-ray and POM data, in fact samples SM and PM scans show
492 some geometrical features like cuts or planes that suggests the presence of crystalline
493 structures even on the sample surfaces. In sample RM, this feature is much less evident
494 and it is completely lost in CM confirming that this sample possesses the loosest structure.

495

496 **4.3 Final discussion**

497 If organogels based on vegetable oils are considered, the onset of crystallisation
498 temperature, T_{co} , decreases with decreasing IFT of the solvent and with increasing ε'_r .
499 Moreover, at a fixed temperature value lower than T_{co} , complex modulus decreases when
500 polarity increases, as confirmed also by crystallinity degree found by microscopic
501 techniques. Organogels based on non-edible oils exhibit a different behaviour and silicon
502 oil is not gelled by Myverol in the adopted conditions, although its properties (polarity,
503 IFT) are close to those of other solvents.

504 Microstructural investigation, performed with X-ray, POM and AFM, confirmed
505 rheological data evidencing that more structured systems are characterised by larger
506 crystalline order and more interconnected elements, in addition, the X-ray highlighted the

507 formation of different structures, in tested organogels, evidenced by differences in the
508 high angle region and related to differences in MAG crystalline phases.

509 FT-IR spectra showed that in all the investigated systems, gelation, when occurring, is
510 promoted by H-bonding. This result is in agreement with previous data for Myverol,
511 whereas is quite unexpected for policosanol, because the literature data evidenced that
512 gelation in virgin olive oil occurred mainly owing to van der Waals interactions (the
513 presence of H-bonds was detected only for high amount of policosanol added to the oil).

514

515 **5. CONCLUSIONS**

516 This paper aimed at analysing, with different techniques, the influence of the solvent
517 nature on the rheological and physicochemical characteristics of edible organogels
518 prepared with MAGs or fatty alcohols as gelators. In particular, polarity, interfacial
519 tension and viscosity of three commercial vegetable oils (sunflower oil, rice oil and castor
520 oil) made of triglycerides chains were used as physical parameters to be investigated as
521 potential influencers of the deriving organogels. Moreover, two additional non-edible oils
522 (paraffin, made of alkane chains, and silicon oil based on chains containing alternating
523 silicon and oxygen atoms) significantly different from edible ones, were also studied to
524 assess the behaviour of used edible gelators in solvents with important differences in
525 chemical nature with respect to vegetable ones.

526 It was observed that when oils with similar chemical nature are considered, a relation
527 seems present among different oil and organogel properties. For instance in vegetable oils
528 made of triglycerides chains, interfacial tension, IFT, increases monotonously with
529 decreasing dielectric constant ϵ'_r , which gives, in turn, a measure of oil polarity; moreover

530 onset of crystallization and complex modulus of organogels are related to ε'_r (and
531 therefore to other oil properties). On the contrary relevant changes in chemical nature (as
532 those occurring when passing from triglycerides to siloxanes) yield to a different
533 dependence of organogel characteristics on oil properties. Therefore few physical
534 parameters, such as polarity, are useful to compare the behaviour of a solvent during
535 gelation only when materials with similar chemical nature are used.

536 Finally, it is worth noticing the important ability of policosanol to act as an organogelator
537 also in oils of a chemical nature quite different from triglycerides, in fact, unlike Myverol,
538 it was able to gel silicon oil.

539

540 **ACKNOWLEDGEMENTS**

541 The authors are grateful to Dr. Y. Marchesano for carrying out the experimental tests, to
542 Prof. N. Scaramuzza (University of Calabria) for impedance measurements and to Dr. I
543 Muzzalupo (CREA-OLI) for fatty acid profiles. Thanks are also due, for its financial
544 support, to project “POR Calabria FESR FSE 2014-2020 “Fat for Fit” funded by *Regione*
545 *Calabria, Azione 1.2.2*”

546 **TABLES CAPTIONS**

547

548 Table 1 Physical properties of oils; SFAs, saturated fatty acids, MUFAs,
549 Monounsaturated fatty acids and PUFAs, Polyunsaturated fatty acids percentages for
550 vegetable oils are also listed.

551 Table 2. ID and qualitative composition of organogels (organogelator amount is 5
552 % w/w for all samples). T_{co} , T_g and the viscosity of the pure solvent evaluated at T_g (μ_{T_g}
553 solvent) are given.

554

555 FIGURES CAPTIONS

556 Figure 1 Dynamic temperature ramp tests at 1 Hz of organogels, in terms of
557 complex modulus, G^* , (a) and phase angle, δ (b). In the legend SM is the organogel
558 produced with SO as the solvent, CM is Castor oil organogel, RM is Rice oil organogel,
559 PM is Paraffin Oil organogel and SiM is Silicon oil organogel. All curves shown in this
560 graphs are related to organogels produced with monoglycerides as gelators.

561 Figure 2 Trend of interfacial tension IFT (full circles) and relative dielectric
562 constant ϵ'_r (open circles) of solvents expressed as a function of onset of crystallisation
563 Temperature, T_{co} , calculated for the corresponding organogel. IFT and ϵ'_r are evaluated
564 at room temperature.

565 Figure 3 Dimensionless complex modulus G_s^* at T_{10} , i.e. 10°C below T_{co} , (eq. 2,
566 full circles) and δ (empty circles) *versus* relative dielectric constant ϵ'_r of the
567 corresponding oil solvent evaluated at room temperature.

568 Figure 4 Dynamic temperature ramp tests of silicon oil organogels produced with
569 policosanol (SiP, purple circle) and monoglycerides (SiM, red triangle). Complex
570 modulus (full symbols) and phase angle (open symbols) are shown.

571 Figure 5 FTIR spectra of pure silicon oil (SiO) and organogels produced with
572 policosanol (SiP) and monoglycerides (SiM). Spectra were obtained at room temperature.

573 Figure 6 Peak Area corresponding to the OH vibrational modes founded in FT-IR
574 spectra at approximately 3500 cm^{-1} . Grey region highlights the area of the peak found in
575 PO spectrum, for differentiating this mineral oil from the others deriving from plant
576 sources. All data were obtained at room temperature.

577 Figure 7 X Ray diffraction: spectra are vertically shifted with respect to each other
578 for clarity. Spectra were obtained at room temperature

579 Figure 8 Polarised Light Microscopy (POM) images of a) Sunflower Oil organogel
580 (SM), b) Rice Oil organogel (RM), c) Paraffin Oil organogel (PM), d) Castor Oil
581 organogel (CM). All organogels were structured with monoglycerides and micrographs
582 were taken at room temperature.

583 Figure 9 Atomic Force Microscopy (AFM) images of a) Sunflower Oil organogel
584 (SM), b) Rice Oil organogel (RM), c) Paraffin Oil organogel (PM), d) Castor Oil
585 organogel (CM). All organogels were structured with monoglycerides and images were
586 taken at room temperature.

587

588 **References**

- 589 Azizian, H. & Kramer, J. K. G. (2005) A rapid method for the quantification of fatty acids
590 in fats and oils with emphasis on trans fatty acids using Fourier transform near infrared
591 spectroscopy (FT-NIR). *Lipids*, 40(8), 855-867.
- 592 Barsoukov, E. & MacDonald, J. R. (eds) (2005) *Impedance Spectroscopy: Theory,*
593 *Experiment, and Applications*, 2nd ed. edition. Hoboken, New Jersey: John Wiley and
594 Science Inc.
- 595 Bot, A. & Agterof, W. G. M. (2006) Structuring of edible oils by mixtures of γ -oryzanol
596 with β -sitosterol or related phytosterols. *Journal of the American Oil Chemists' Society*,
597 83(6), 513-521.
- 598 Bot, A., den Adel, R. & Roijers, E. C. (2008) Fibrils of γ -Oryzanol + β -Sitosterol in
599 Edible Oil Organogels. *Journal of the American Oil Chemists' Society*, 85(12), 1127-
600 1134.
- 601 Brulls, M., Folestad, S., Sparen, A., Rasmuson, A. & Salomonsson, J. (2007) Applying
602 spectral peak area analysis in near-infrared spectroscopy moisture assays. *Journal of*
603 *Pharmaceutical and Biomedical Analysis*, 44(1), 127-136.
- 604 Calligaris, S., Da Pieve, S., Arrighetti, G. & Barba, L. (2010) Effect of the structure of
605 monoglyceride-oil-water gels on aroma partition. *Food Research International*, 43(3),
606 671-677.
- 607 Calligaris, S., Mirolo, G., Da Pieve, S., Arrighetti, G. & Nicoli, M. C. (2014) Effect of
608 Oil Type on Formation, Structure and Thermal Properties of gamma-oryzanol and beta-
609 sitosterol-Based Organogels. *Food Biophysics*, 9(1), 69-75.
- 610 Casale, M., Oliveri, P., Casolino, C., Sinelli, N., Zunin, P., Armanino, C., Forina, M. &
611 Lanteri, S. (2012) Characterisation of PDO olive oil Chianti Classico by non-selective
612 (UV-visible, NIR and MIR spectroscopy) and selective (fatty acid composition)
613 analytical techniques. *Analytica Chimica Acta*, 712, 56-63.

- 614 Chaves, K. F., Barrera-Arellano, D. & Ribeiro, A. P. B. (2017) Potential application of
615 lipid organogels for food industry. *Food Research International*.
- 616 Chen, C. H. & Terentjev, E. M. (2009) Aging and Metastability of Monoglycerides in
617 Hydrophobic Solutions. *Langmuir*, 25(12), 6717-6724.
- 618 Co, E. D. & Marangoni, A. G. (2012) Organogels: An Alternative Edible Oil-Structuring
619 Method. *Journal of the American Oil Chemists Society*, 89(5), 749-780.
- 620 de Vries, A., Gomez, Y. L., van der Linden, E. & Scholten, E. (2017) The effect of oil
621 type on network formation by protein aggregates into oleogels. *Rsc Advances*, 7(19),
622 11803-11812.
- 623 Galtier, O., Dupuy, N., Le Dréau, Y., Ollivier, D., Pinatel, C., Kister, J. & Artaud, J.
624 (2007) Geographic origins and compositions of virgin olive oils determined by
625 chemometric analysis of NIR spectra. *Analytica Chimica Acta*, 595(1), 136-144.
- 626 Grompone, M. A. (2011) Sunflower Oil, *Vegetable Oils in Food Technology*Wiley-
627 Blackwell, 137-167.
- 628 Hwang, H. S., Singh, M., Winkler-Moser, J. K., Bakota, E. L. & Liu, S. X. (2014)
629 Preparation of Margarines from Organogels of Sunflower Wax and Vegetable Oils.
630 *Journal of Food Science*, 79(10), C1926-C1932.
- 631 Johnson, W. (2007) Final report on the safety assessment of ricinus communis (castor)
632 seed oil, hydrogenated castor oil, glyceryl ricinoleate, glyceryl ricinoleate SE, ricinoleic
633 acid, potassium ricinoleate, sodium ricinoleate, zinc ricinoleate, cetyl ricinoleate, ethyl
634 ricinoleate, glycol ricinoleate, isopropyl ricinoleate, methyl ricinoleate, and octyldodecyl
635 ricinoleate. *International Journal of Toxicology*, 26, 31-77.
- 636 Kim, J.-Y., Lee, J. H., Jeong, D.-Y., Jang, D.-K., Seo, T.-R. & Lim, S.-T. (2015)
637 Preparation and characterization of aqueous dispersions of dextrin and policosanol
638 composites. *Carbohydrate Polymers*, 121, 140-146.

- 639 Kochhar, S. P. (2011) Minor and Speciality Oils, *Vegetable Oils in Food*
640 *Technology*Wiley-Blackwell, 291-341.
- 641 Lupi, F., Gabriele, D., de Cindio, B., Sanchez, M. & Gallegos, C. (2011) A rheological
642 analysis of structured water-in-olive oil emulsions. *Journal of Food Engineering*, 107(3-
643 4), 296-303.
- 644 Lupi, F. R., Gabriele, D., Facciolo, D., Baldino, N., Seta, L. & de Cindio, B. (2012) Effect
645 of organogelator and fat source on rheological properties of olive oil-based organogels.
646 *Food Research International*, 46(1), 177-184.
- 647 Lupi, F. R., Gabriele, D., Greco, V., Baldino, N., Seta, L. & de Cindio, B. (2013) A
648 rheological characterisation of an olive oil/fatty alcohols organogel. *Food Research*
649 *International*, 51(2), 510-517.
- 650 Lupi, F. R., Greco, V., Baldino, N., de Cindio, B., Fischer, P. & Gabriele, D. (2016) The
651 effects of intermolecular interactions on the physical properties of organogels in edible
652 oils. *Journal of Colloid and Interface Science*, 483, 154-164.
- 653 Lupi, F. R., Shakeel, A., Greco, V., Baldino, N., Calabrò, V. & Gabriele, D. (2017)
654 Organogelation of extra virgin olive oil with fatty alcohols, glyceryl stearate and their
655 mixture. *LWT - Food Science and Technology*, 77, 422-429.
- 656 Marangoni, A. G. & Garti, N. (2011) 1 - An Overview of the Past, Present, and Future of
657 Organogels, *Edible Oleogels*AOCS Press, 1-17.
- 658 Marangoni, A. G., Idziak, S. H. J., Vega, C., Batte, H., Ollivon, M., Jantzi, P. S. & Rush,
659 J. W. E. (2007) Encapsulation-structuring of edible oil attenuates acute elevation of blood
660 lipids and insulin in humans. *Soft Matter*, 3(2), 183.
- 661 Morales-Rueda, J. A., Dibildox-Alvarado, E., Charo-Alonso, M. A., Weiss, R. G. & Toro-
662 Vazquez, J. F. (2009) Thermo-mechanical properties of candelilla wax and dotriacontane

663 organogels in safflower oil. *European Journal of Lipid Science and Technology*, 111(2),
664 207-215.

665 Nouredдини, H., Teoh, B. C. & Davis Clements, L. (1992) Viscosities of vegetable oils
666 and fatty acids. *Journal of the American Oil Chemists Society*, 69(12), 1189-1191.

667 Ojijo, N. K., Neeman, I., Eger, S. & Shimoni, E. (2004) Effects of monoglyceride content,
668 cooling rate and shear on the rheological properties of olive oil/monoglyceride gel
669 networks. *Journal of the Science of Food and Agriculture*, 84(12), 1585-1593.

670 Parolo, M. E., Savini, M. C. & Loewy, R. M. (2017) Characterization of soil organic
671 matter by FT-IR spectroscopy and its relationship with chlorpyrifos sorption. *Journal of*
672 *Environmental Management*, 196, 316-322.

673 Quinchia, L. A., Delgado, M. A., Franco, J. M., Spikes, H. A. & Gallegos, C. (2012) Low-
674 temperature flow behaviour of vegetable oil-based lubricants. *Industrial Crops and*
675 *Products*, 37(1), 383-388.

676 Sawalha, H., Margry, G., den Adel, R., Venema, P., Bot, A., Floter, E. & van der Linden,
677 E. (2013) The influence of the type of oil phase on the self-assembly process of gamma-
678 oryzanol plus beta-sitosterol tubules in organogel systems. *European Journal of Lipid*
679 *Science and Technology*, 115(3), 295-300.

680 Schaink, H. M., van Malssen, K. F., Morgado-Alves, S., Kalnin, D. & van der Linden, E.
681 (2007) Crystal network for edible oil organogels: Possibilities and limitations of the fatty
682 acid and fatty alcohol systems. *Food Research International*, 40(9), 1185-1193.

683 Seta, L., Baldino, N., Gabriele, D., Lupi, F. R. & de Cindio, B. (2012) The effect of
684 surfactant type on the rheology of ovalbumin layers at the air/water and oil/water
685 interfaces. *Food Hydrocolloids*, 29(2), 247-257.

686 Seta, L., Baldino, N., Gabriele, D., Lupi, F. R. & de Cindio, B. (2014) Rheology and
687 adsorption behaviour of beta-casein and beta-lactoglobulin mixed layers at the sunflower

688 oil/water interface. *Colloids and Surfaces a-Physicochemical and Engineering Aspects*,
689 441, 669-677.

690 Suzuki, M., Nakajima, Y., Yumoto, M., Kimura, M., Shirai, H. & Hanabusa, K. (2003)
691 Effects of hydrogen bonding and van der Waals interactions on organogelation using
692 designed low-molecular-weight gelators and gel formation at room temperature.
693 *Langmuir*, 19(21), 8622-8624.

694 Toro-Vazquez, J. F., Mauricio-Perez, R., Gonzalez-Chavez, M. M., Sanchez-Becerril,
695 M., Ornelas-Paz, J. D. & Perez-Martinez, J. D. (2013) Physical properties of organogels
696 and water in oil emulsions structured by mixtures of candelilla wax and monoglycerides.
697 *Food Research International*, 54(2), 1360-1368.

698 van Esch, J. H. & Feringa, B. L. (2000) New Functional Materials Based on Self-
699 Assembling Organogels: From Serendipity towards Design. *Angewandte Chemie*
700 *International Edition*, 39(13), 2263-2266.

701 Wang, T. (2011) Soybean Oil, *Vegetable Oils in Food Technology*Wiley-Blackwell, 59-
702 105.

703 Wu, S., Gao, J., Emge, T. J. & Rogers, M. A. (2013) Influence of solvent on the
704 supramolecular architectures in molecular gels. *Soft Matter*, 9(25), 5942-5950.

705 Wu, Y. P., Wu, S., Zou, G. & Zhang, Q. J. (2011) Solvent effects on structure,
706 photoresponse and speed of gelation of a dicholesterol-linked azobenzene organogel. *Soft*
707 *Matter*, 7(19), 9177-9183.

708 Zhu, G. Y. & Dordick, J. S. (2006) Solvent effect on organogel formation by low
709 molecular weight molecules. *Chemistry of Materials*, 18(25), 5988-5995.

710 Zweep, N., Hopkinson, A., Meetsma, A., Browne, W. R., Feringa, B. L. & van Esch, J.
711 H. (2009) Balancing Hydrogen Bonding and van der Waals Interactions in Cyclohexane-
712 Based Bisamide and Bisurea Organogelators. *Langmuir*, 25(15), 8802-8809.

Table 1

713

714

Oil type	Name	μ (Pa s) (25°C, $\dot{\gamma} = 10 \text{ s}^{-1}$)	IFT (mN/m)	ϵ'_r (-) (0.1 kHz)	SFAs (%)	MUFAs (%)	PUFAs (%)
Sunflower	SO	0.052±0.003	24±1	3.2±0.2	9.4	28.3	62.3
Castor	CO	0.72±0.02	12.9±0.3	4.7±0.2	5.4	83.35	11.25
Rice	RO	0.062±0.001	21.8±0.2	3.8±0.2	22.5	44	33.5
Paraffin	PO	0.082±0.007	32±2	2.9±0.1	-	-	-
Silicon	SiO	0.015±0.001	37.9±0.4	2.9±0.1	-	-	-

715

Table 2

Organogel	Oil	Organogelator	T_{co} (°C)	T_g (°C)	μT_{g solvent} (Pa s)
SM	SO	Myverol	50±1	48±1	0.022±0.003
CM	CO	Myverol	29.8±0.3	28.5±0.2	0.57±0.02
RM	RO	Myverol	46.6±0.6	43±2	0.033±0.001
PM	PO	Myverol	59.7±0.3	57±1	0.016±0.001
SiM	SiO	Myverol	-	-	-
SiP	SiO	Policosanol	79.2±0.3	74.2±0.2	0.009±0.001

716

Figure 1a

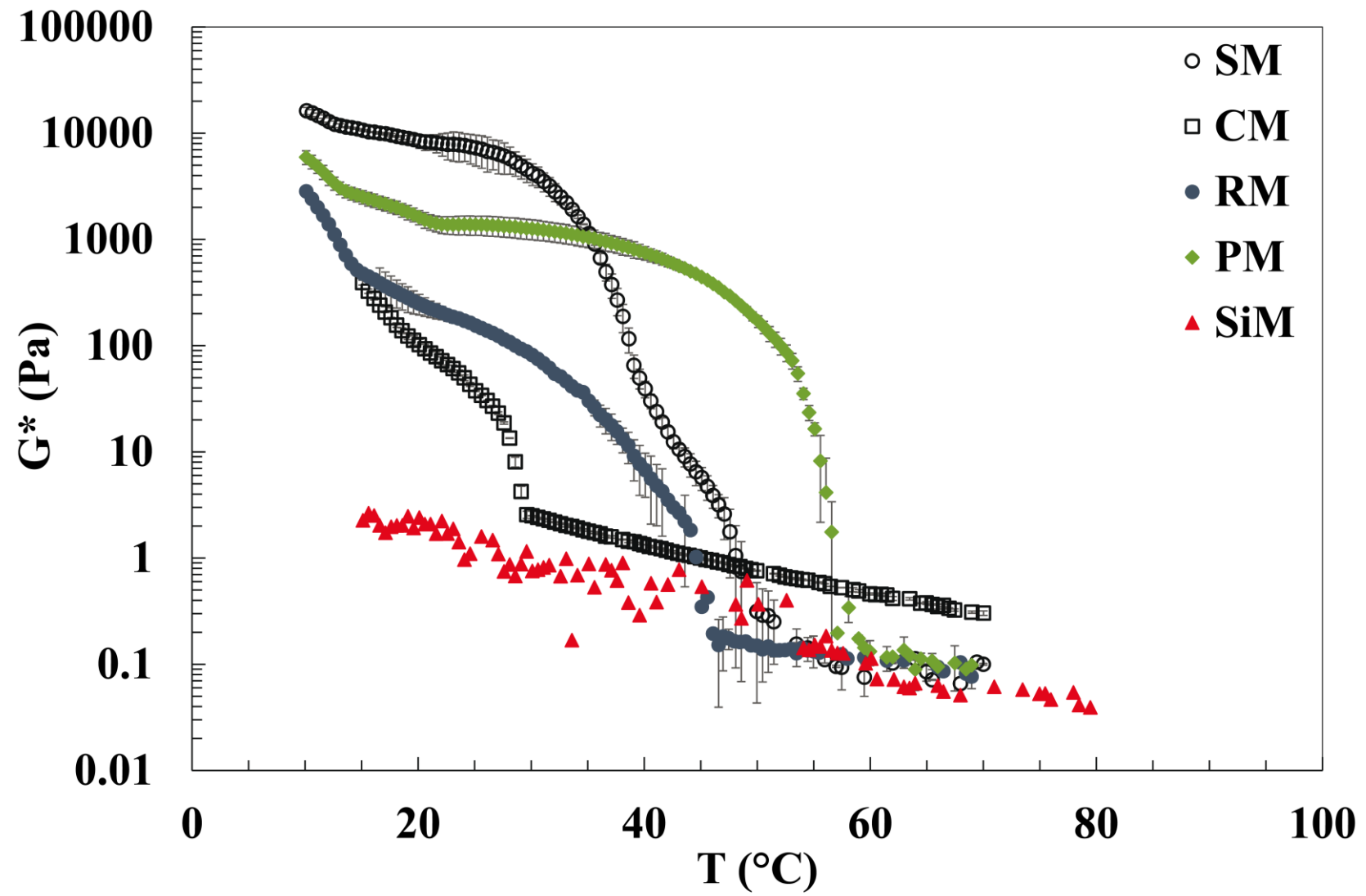


Figure 1b

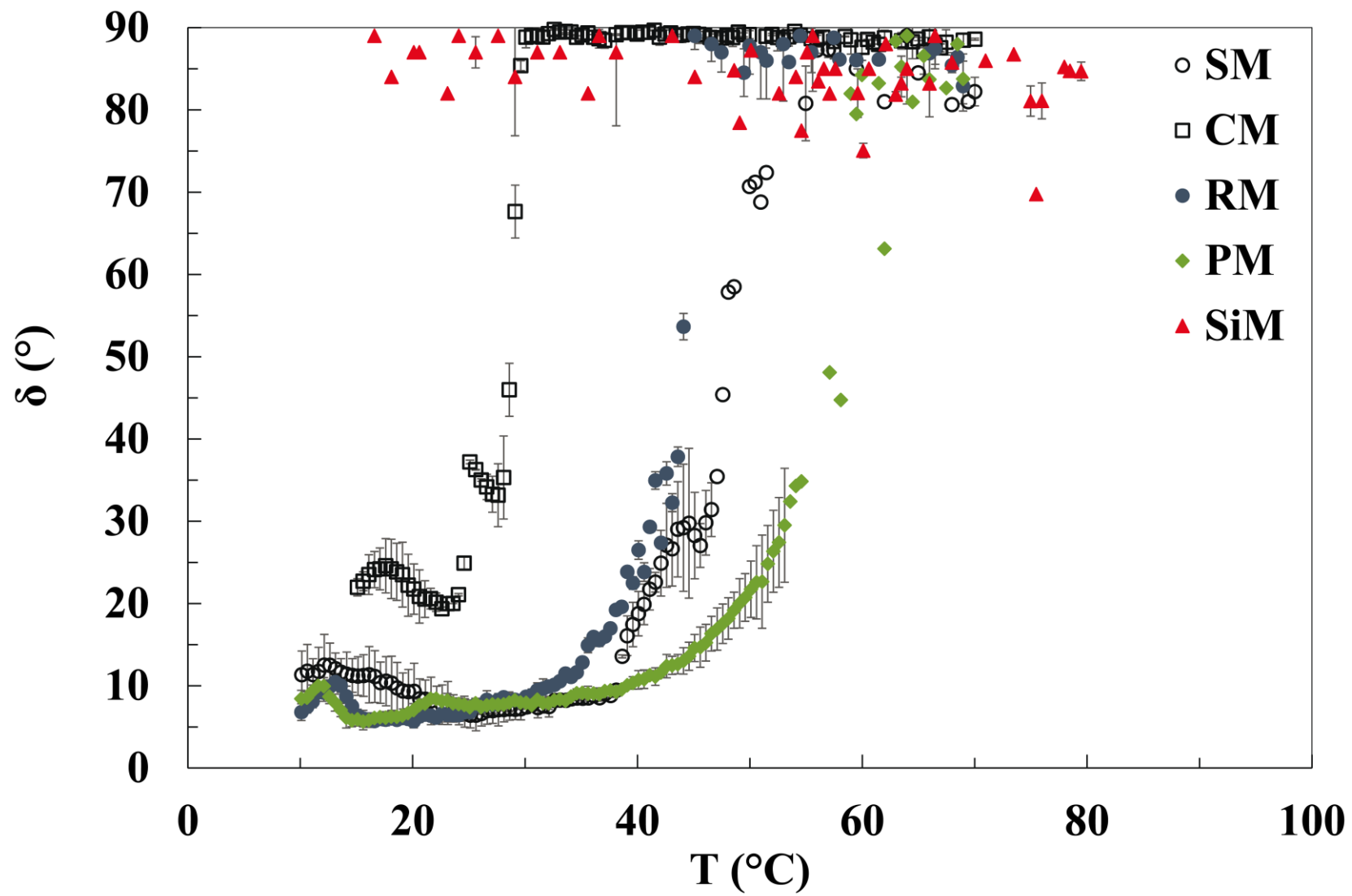


Figure 2

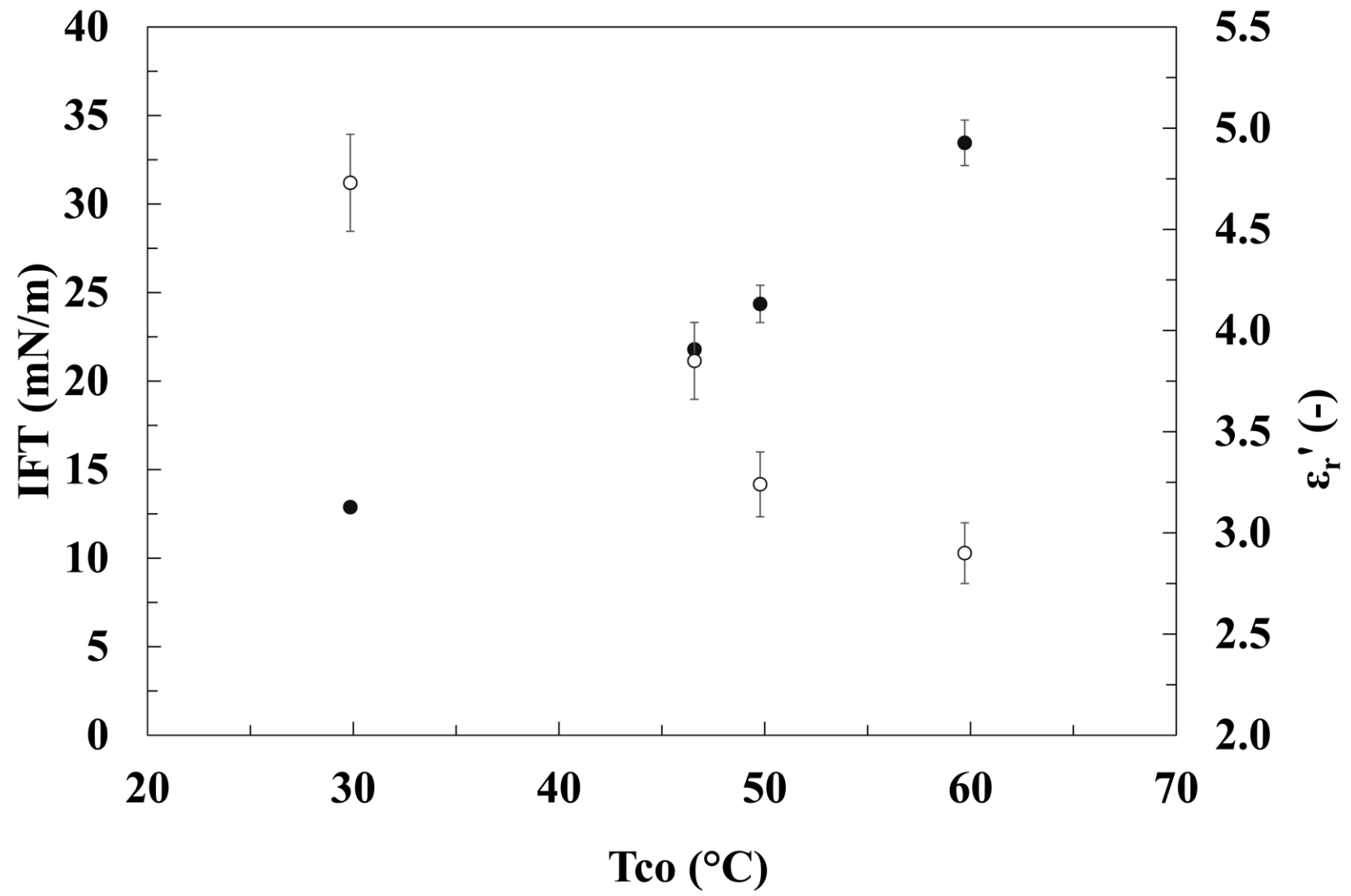


Figure 3

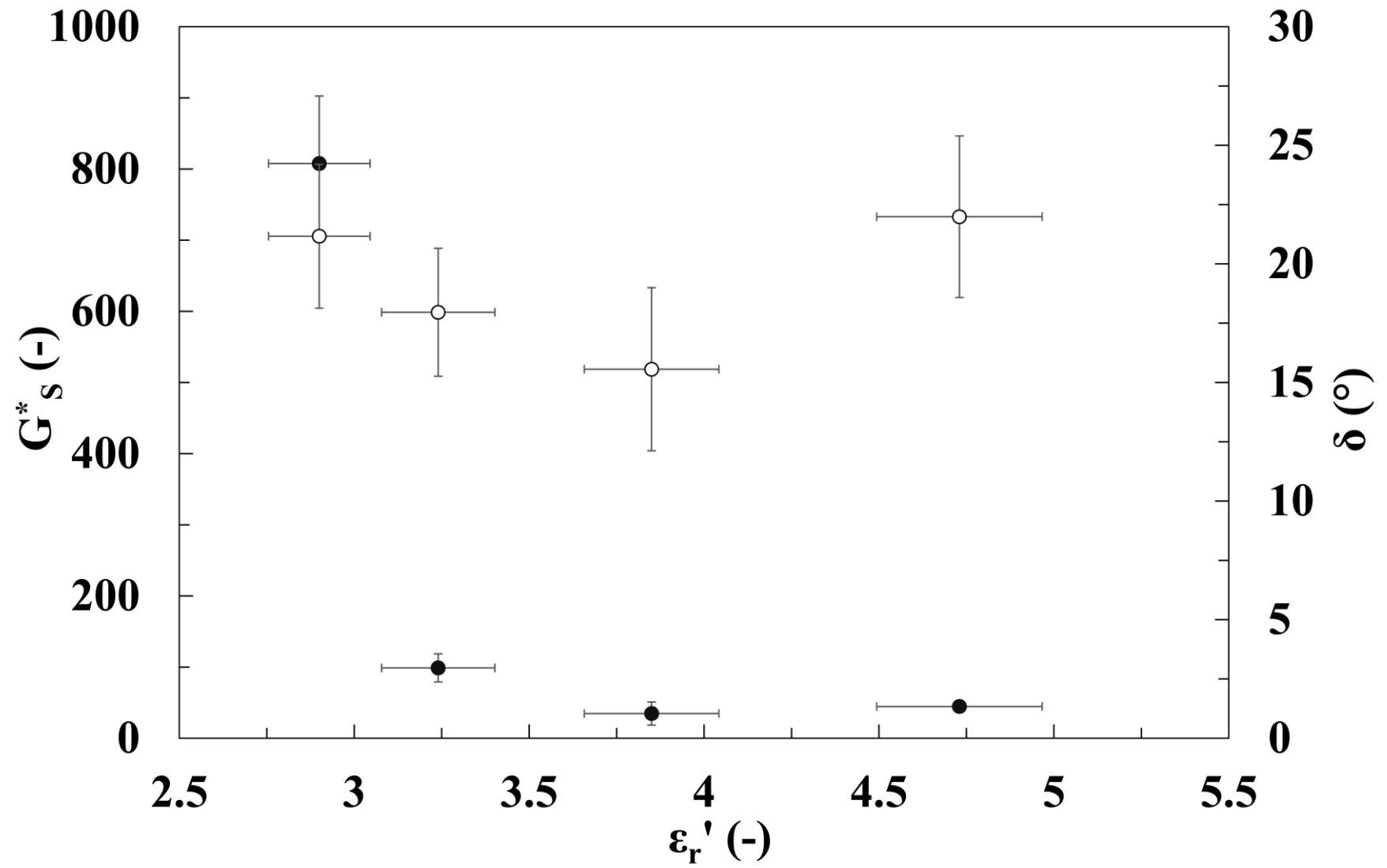


Figure 4

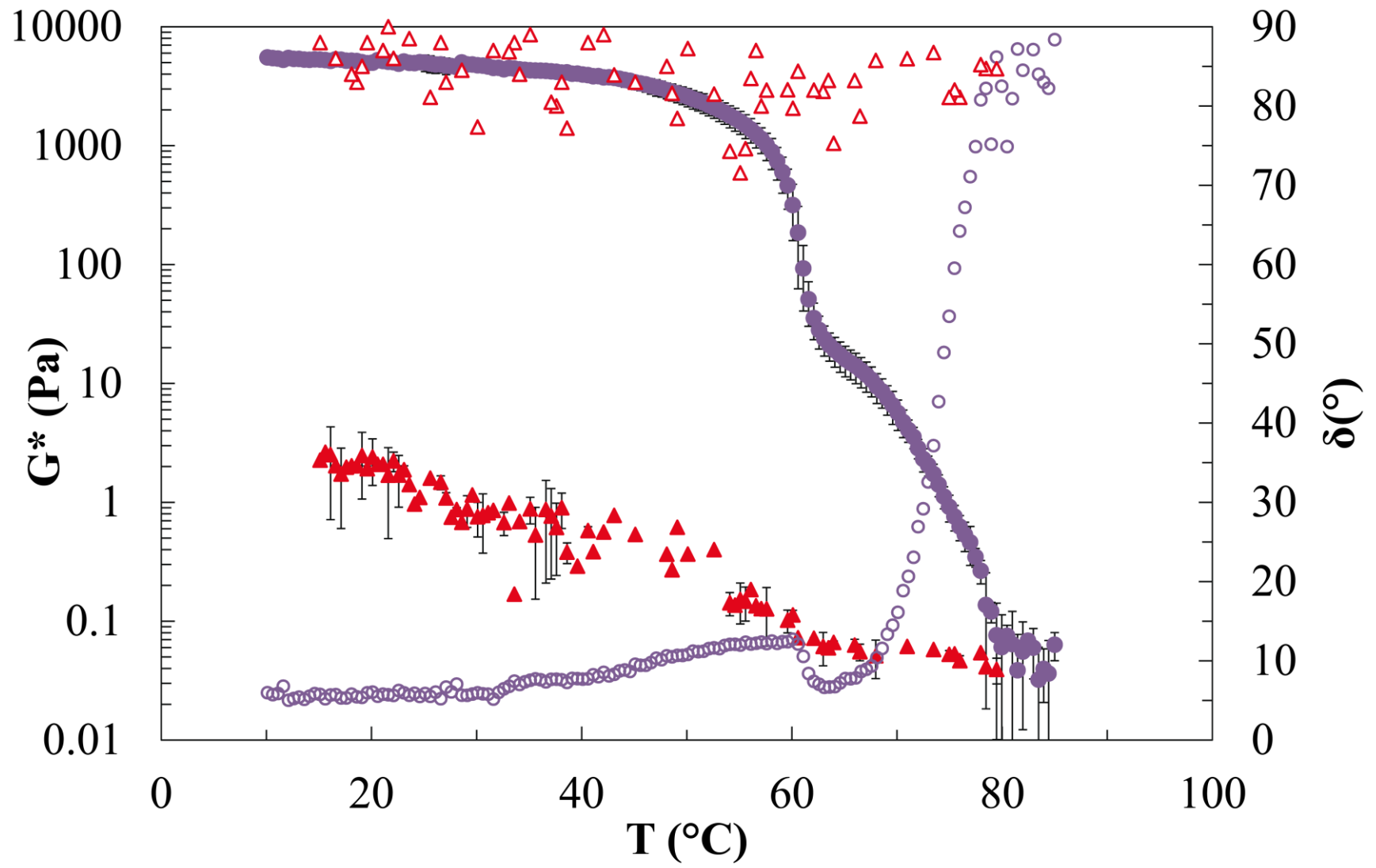


Figure 5

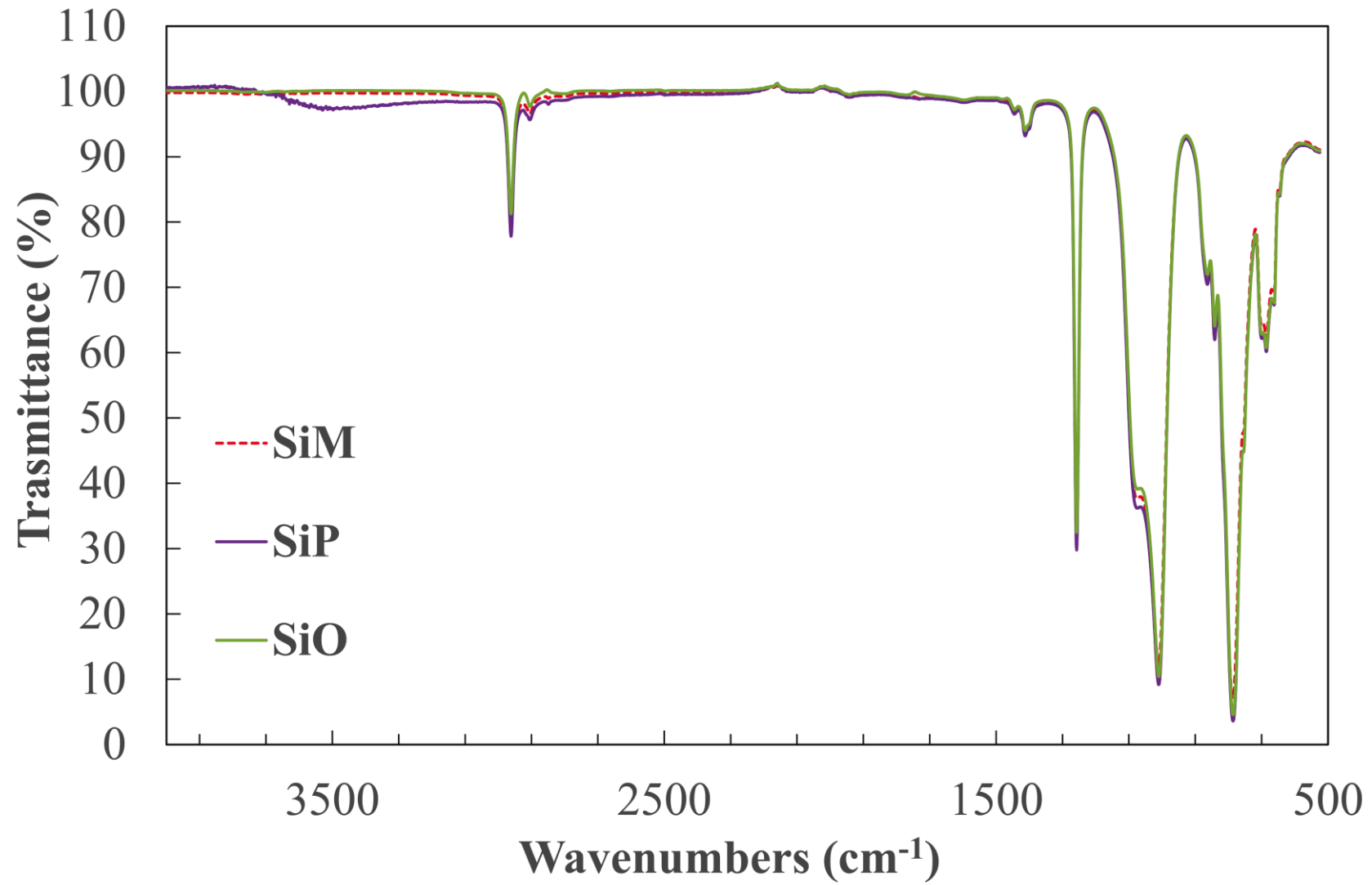


Figure 6

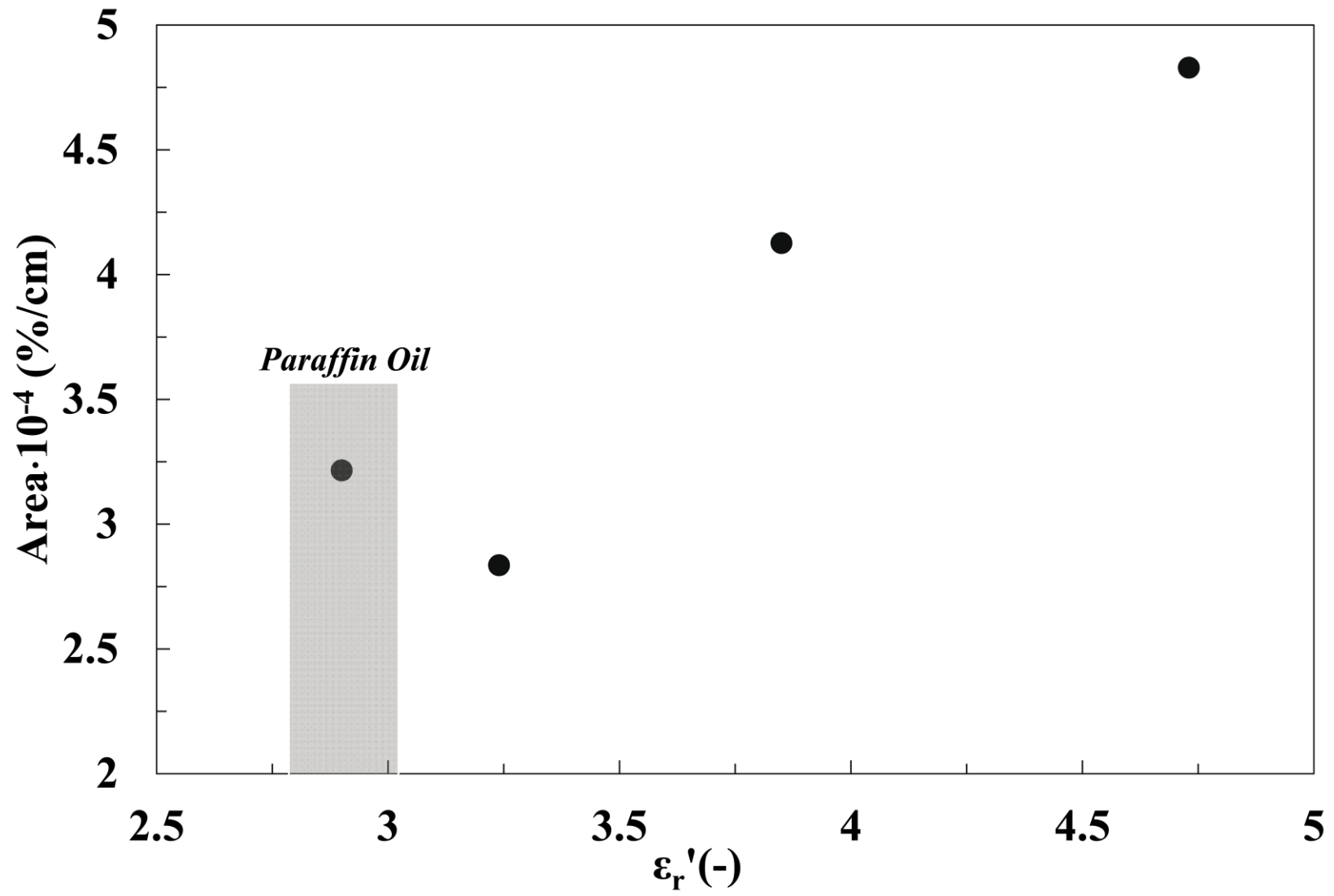


Figure 7

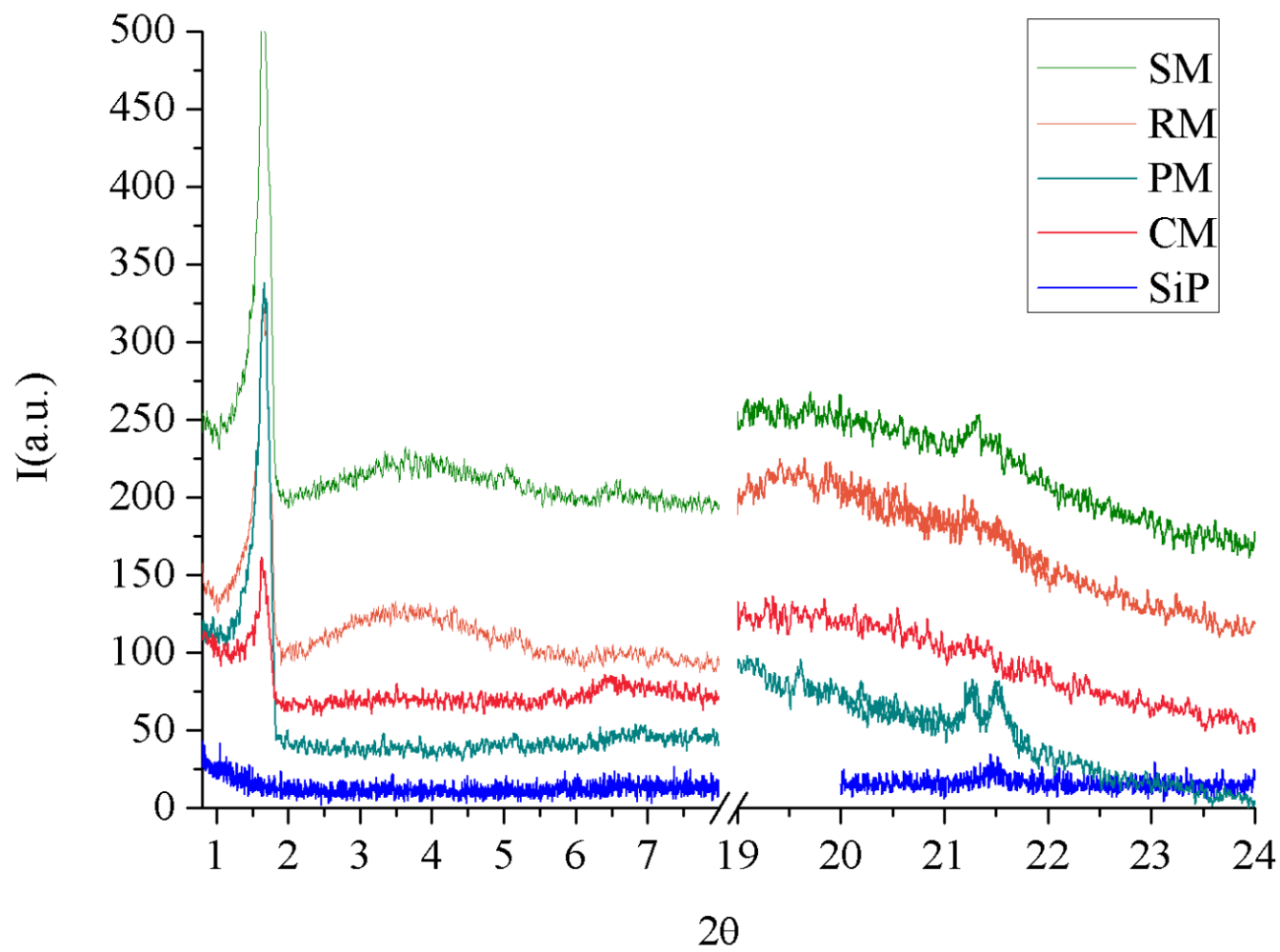
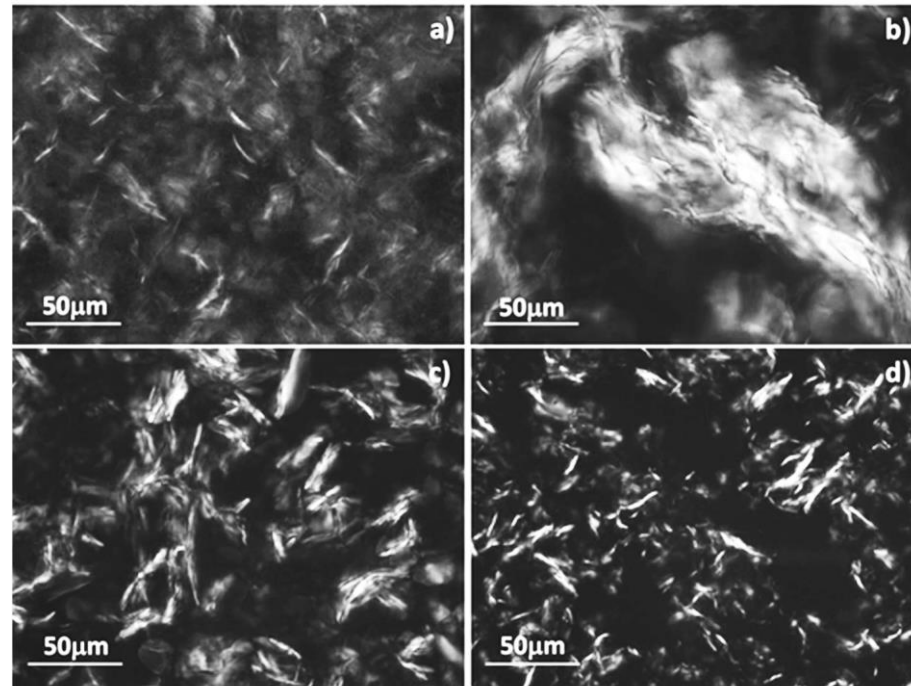


Figure 8



725

Figure 9

